

# Dalton Transactions

Accepted Manuscript



This is an *Accepted Manuscript*, which has been through the Royal Society of Chemistry peer review process and has been accepted for publication.

*Accepted Manuscripts* are published online shortly after acceptance, before technical editing, formatting and proof reading. Using this free service, authors can make their results available to the community, in citable form, before we publish the edited article. We will replace this *Accepted Manuscript* with the edited and formatted *Advance Article* as soon as it is available.

You can find more information about *Accepted Manuscripts* in the [Information for Authors](#).

Please note that technical editing may introduce minor changes to the text and/or graphics, which may alter content. The journal's standard [Terms & Conditions](#) and the [Ethical guidelines](#) still apply. In no event shall the Royal Society of Chemistry be held responsible for any errors or omissions in this *Accepted Manuscript* or any consequences arising from the use of any information it contains.

Cite this: DOI: 10.1039/c0xx00000x

www.rsc.org/xxxxxx

ARTICLE TYPE

## Magnetic and conductive study on a stable defective extended cobalt atom chain

Wen-Zhen Wang,<sup>\*a</sup> Yang Wu,<sup>a</sup> Rayyat H. Ismayilov,<sup>b</sup> Juao-Hui Kuo,<sup>c</sup> Chen-Yu Yeh,<sup>d</sup> Hsuan-Wei Lee,<sup>d</sup> Ming-Dung Fu,<sup>c</sup> Chun-hsien Chen,<sup>\*c</sup> Gene-Hsiang Lee,<sup>c</sup> and Shie-Ming Peng<sup>\*c</sup>

<sup>5</sup> Received (in XXX, XXX) Xth XXXXXXXXX 20XX, Accepted Xth XXXXXXXXX 20XX

DOI: 10.1039/b000000x

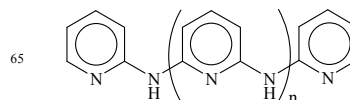
Two pentacobalt(II) EMACs were synthesized. A pyrazine-modulated tripyridyldiamine resulted in a EMAC with fully delocalized Co-Co bonds along molecules. From a pyrazine- and naphthyridine-containing ligand, a defective cobalt linear EMAC with an 8-coordinated cobalt(II) in the center was obtained for the first time. Electrochemistry study on the defective pentacobalt chain compound showed redox peaks at  $E_{1/2} = -1.00, +0.76, \text{ and } +0.98 \text{ V}$  (versus  $E_{\text{Ag/AgCl}}$ ), indicating that it is quite stable and very resistant to both oxidation and reduction. Research on magnetism revealed that the fully delocalized Co EMAC is a spin mixture, and the defective cobalt EMAC showed a high-spin mononuclear cobalt(II) behaviour with a magnetic moment of  $2.63 \mu_{\text{B}}$  per molecule at room temperature. Measurement on molecular electric conductance by STM showed single-molecular resistance of  $15.4 (\pm 3.1) \text{ M}\Omega$  for defective and  $12.3 (\pm 2.6) \text{ M}\Omega$  for delocalized pentacobalt complexes.

### Introduction

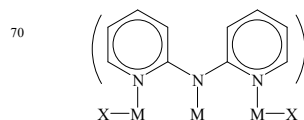
Over the past decades increasing attention has been paid to molecular electronics. Linear metal string complexes with metal-metal interaction showed potential applications as molecular devices such as molecular wires, switches and rectifiers.<sup>[1]</sup> Also called extended metal-atom chain (EMAC), the typical structure of this family includes a linear metal chain helically wrapped by four deprotonated oligo- $\alpha$ -pyridylamido ligands (Scheme 1), with the pyridine nitrogen atoms and amido nitrogen atoms all coordinated in a *syn*-form (Scheme 2). STM (scanning tunnelling microscope) studies revealed that EMACs exhibited superior electronic conductance, which made the finest metal wire consisting of single metal-atom line and wrapped with organic ligands as the insulating shroud.<sup>[1]</sup> The first EMAC,  $[\text{Ni}_3(\text{dpa})_4\text{Cl}_2]$ , was synthesized by Hurley in 1968.<sup>[2]</sup> It was not until 1991, however, that its structure was correctly elaborated by Aduldecha and Hathaway through X-ray crystallography (Scheme 2,  $\text{M} = \text{Ni}^{2+}$ ,  $\text{X} = \text{Cl}^-$ ).<sup>[3]</sup> Subsequent development on EMACs, delivered by Cotton and coworkers and Peng's group, has focused on EMACs of oligo- $\alpha$ -pyridylamido ligands.<sup>[4-9]</sup> In recent years we have developed a series of modification to the prototypical oligo- $\alpha$ -pyridylamido ligands and expanded the variety and number of metal atoms in EMACs, leading to novel synthetic strategies, innovative structures, and fascinating properties.<sup>[6-8]</sup> The modified ligands, mainly by the replacement of pyridyl ring(s) with other group(s), comprise the following substitutions: (1) non-coordinating groups, *e.g.*, benzene, toluenesulfonyl or methylsulfonyl groups,<sup>[4]</sup> containing less coordination positions than the prototypical ligands, subsequently, giving even-numbered anionic or neutral EMACs

of  $\text{M}^{2+}$  without anionic axial ligands; (2) electron-donor or acceptor groups, such as alkyl substituents, pyrazine, or pyrimidine,<sup>[6]</sup> which evolve a broad range of unprecedented ligands with improved reactivity to render novel EMACs with redox properties very different from those of the corresponding prototypical ones; (3) naphthyridine group,<sup>[1c,7]</sup> containing less amido anions than that of oligo- $\alpha$ -pyridylamido ligands, giving cationic EMACs which further afford the reduced forms. This family of modulated ligands shows very attractive properties. For example, naphthyridine-modulated ligands direct the formation of mixed valence units  $[\text{Ni}_2(\text{napy})_4]^{3+}$ . The di-nickel unit exhibits features of electron delocalisation, including shorter nickel-nickel bond, more redox waves in the electrochemical potential window, and higher conductance than its prototypical form.<sup>[7d]</sup>

**Scheme 1.** Prototypical ligands of oligo- $\alpha$ -pyridylamines for EMACs.



**Scheme 2.** Typical structure of trimetal EMACs.



Previous STM investigation revealed that the conductance of EMACs is correlated strongly with the strengths of metal-metal bonds and the presence of electron delocalization along the metal-atom chain.<sup>[1a]</sup> Of particular note, all cobalt EMACs that

have been reported exhibit nonzero Co-Co bond order and delocalized electrons.<sup>[10]</sup> The magnetism of cobalt EMACs is also a fascinating topic. Tricobalt EMACs have both symmetrical and unsymmetrical structures, offering very rare examples of bond-stretch isomers. The complexes have a doublet ground state at low temperature and undergo spin crossover process.<sup>[10d,10e]</sup> The penta- and reduced hexacobalt EMACs have a doublet ground state with a temperature-independent magnetic moment.<sup>[7b,10c]</sup> Spin-equilibrium takes place for pyrazine-modulated penta- and heptacobalt EMACs and intermediate magnetic moments between doublet and quartet spin states have been observed.<sup>[6b,6d]</sup> With the rich magnetic behaviours and unique molecular and electronic structures, cobalt EMACs are one of the most challenging systems. In order to explore cobalt EMACs of different structures and redox property, and to understand their formation, the mechanism of magnetic coupling and electric conductance, we designed and synthesized new modulated tripyridyldiamine ligands. Unexpectedly, through a new ligand containing pyrazine and naphthyridine (**1**, Scheme 1), a pentacobalt EMAC (**2**, Figure 1) with one Co centre missing in the presumably six-coordination sites was obtained for the first time. Reported herein are the synthesis, the magnetic behaviour and electric conductance this defective cobalt EMAC complex.

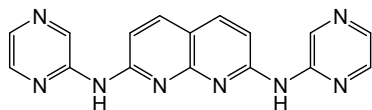
## Results and Discussion

### Syntheses

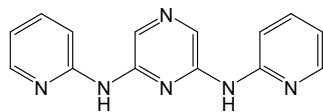
The ligands  $N^2,N^7$ -di(pyrazin-2-yl)-1,8-naphthyridine-2,7-diamine ( $H_2dpznda$ ) (**1**) and  $N,N'$ -di(pyridin-2-yl)pyrazine-2,6-diamine ( $H_2dppzda$ ) (**3**) (Scheme 3) were synthesized on the basis of the Buchwald's palladium-catalyzed procedures *via* the cross-coupling of halogenide and amine, and characterized by IR,  $^1H$  NMR and MS (FAB). The EMACs,  $[Co_5(\mu_5-dpznda)_4(NCS)_2]$  (**2**) and  $[Co_5(\mu_5-dppzda)_4(NCS)_2]$  (**4**), were synthesized by the reaction of anhydrous  $CoCl_2$  with **1** or **3** at high temperature (180–200 °C) employing naphthalene as solvent and  $Bu^tOK$  as a base to deprotonate the amine group, and after a substitution of axial ligands  $Cl^-$  by  $NCS^-$ .

### Scheme 3.

$N^2,N^7$ -di(pyrazin-2-yl)-1,8-naphthyridine-2,7-diamine ( $H_2dpznda$ ) (**1**)



$N,N'$ -di(pyridin-2-yl)pyrazine-2,6-diamine ( $H_2dppzda$ ) (**3**)



### Structures

The crystal structure of **2** is shown in Fig. 1. Selected bond distances and angles are shown in Table 1. The complex consists of five cobalt(II) atoms in a linear chain with Co–Co–Co angles in the range of 175–180°. There are four equatorial ligands in a molecule, wrapping around the metal string in a *syn-syn* form as

dianion helices. The nitrogen atoms of axial ligands ( $NCS^-$ ) bonded to the terminal metal atoms are collinear with the  $Co_5$  axis.

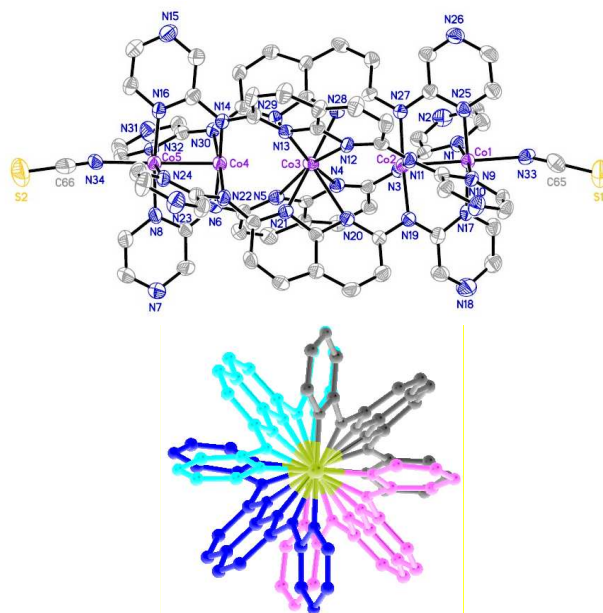


**Fig. 1** (a) ORTEP drawing and (b) a view illustrating the quadruple helix along the metal-chain axis of **2**. Thermal ellipsoids are drawn at the 30% probability level. The hydrogen atoms in the ORTEP and the terminal  $NCS^-$  of Panel b are not shown for clarity. Selected bond distances (Å) for **2**: Co(1)–Co(2) 2.3293(12); Co(2)–Co(3) 3.274(13); Co(3)–Co(4) 3.238(13); Co(4)–Co(5) 2.3365(13); Co(1)– $N_{av}$  1.949(7); Co(2)– $N_{av}$  1.933(6); Co(3)– $N_{av}$  2.308(6); Co(4)– $N_{av}$  1.925(6); Co(5)– $N_{av}$  1.957(6); Co(1)– $N_{NCS}$  2.112(7); Co(5)– $N_{NCS}$  2.100(6); Co(1)–Co(2)–Co(3) 174.69(19); Co(2)–Co(3)–Co(4) 179.18(19); Co(3)–Co(4)–Co(5) 175.51(19);  $N-Co(1)-Co(5)-N$  92.72.

The length of molecule **2** is 20.56 Å, with the  $Co_5$  core length of 11.17 Å. It is noticeable that **2** is hexadentate. Hence, hexametal EMACs are expected as those resulted from analogous ligands of **1**,  $H_2bpyany$  ( $N^2,N^7$ -di(pyridin-2-yl)-1,8-naphthyridine-2,7-diamine) and  $H_2bpmany$  ( $N^2,N^7$ -di(pyrimidin-2-yl)-1,8-naphthyridine-2,7-diamine).<sup>[7]</sup> However, one metal atom in the centre is missing. This is the first example of a cobalt defective EMAC with the absence of one metal atom in the central portion of the metal-atom chain.

At the termini of complex **2**, there are two Co–Co bonds with spacing of 2.3293(13) Å and 2.3365(13) Å for Co(1)–Co(2) and Co(4)–Co(5), respectively, indicative of a metal-metal bond between the cobalt pairs although the values are longer than those of **4** and also longer than the previously reported 2.232–2.286 Å in Co EMACs.<sup>[6b,6d,10]</sup> The central cobalt(II) is separated by a distance of 3.274(13) Å away from Co(2) and by 3.238(13) Å from Co(4). Thus, EMAC **2** is essentially constituted of three parts with two bicobalt(II) units at the terminal and one separated mononuclear  $Co^{2+}$  atom in the centre. The Co–N( $dpznda$ ) bond lengths for the binuclear cobalt atoms are in the range of 1.918(6)–1.965(6) Å. Co– $N_{amido}$  bond distances are the shortest due to the high negative charge density at amido nitrogen atoms, consistent with previously reported cobalt EMACs.<sup>[6b,6d,10]</sup> It is worth noting that the central, separated  $Co^{2+}$  atom is 8-coordinated to all the eight nitrogen atoms of four naphthyridyl moieties. The Co– $N_{napy}$  distances in **2** fall into two groups: four

Table 1. Selected bond lengths (Å) and angles (°) for 2.

Co(1)-Co(2)	2.3293(12)	N(17)-Co(1)-N(9)	88.7(2)	N(21)-Co(3)-N(20)	57.43(19)
Co(1)-N(1)	1.947(6)	N(17)-Co(1)-N(25)	173.7(2)	N(21)-Co(3)-N(29)	124.16(19)
Co(1)-N(9)	1.951(6)	N(17)-Co(1)-N(33)	93.6(2)	N(28)-Co(3)-N(4)	78.9(2)
Co(1)-N(17)	1.940(6)	N(25)-Co(1)-N(33)	92.6(2)	N(28)-Co(3)-N(5)	114.04(19)
Co(1)-N(25)	1.957(6)	N(9)-Co(1)-Co(2)	86.49(16)	N(28)-Co(3)-N(12)	79.20(19)
Co(1)-N(33)	2.112(7)	N(25)-Co(1)-Co(2)	87.20(16)	N(28)-Co(3)-N(13)	90.6(2)
Co(2)-N(3)	1.940(6)	N(33)-Co(1)-Co(2)	179.69(17)	N(28)-Co(3)-N(20)	123.22(19)
Co(2)-N(11)	1.923(6)	N(3)-Co(2)-N(19)	90.5(2)	N(28)-Co(3)-N(21)	170.0(2)
Co(2)-N(19)	1.942(6)	N(11)-Co(2)-N(3)	176.9(2)	N(28)-Co(3)-N(29)	58.31(19)
Co(2)-N(27)	1.927(5)	N(11)-Co(2)-N(19)	89.9(2)	N(29)-Co(3)-N(20)	164.9(2)
Co(3)-N(4)	2.294(6)	N(11)-Co(2)-N(27)	89.8(2)	N(14)-Co(4)-N(6)	177.3(2)
Co(3)-N(5)	2.352(6)	N(27)-Co(2)-N(3)	89.7(2)	N(14)-Co(4)-N(22)	90.5(2)
Co(3)-N(12)	2.340(6)	N(27)-Co(2)-N(19)	176.5(2)	N(14)-Co(4)-N(30)	90.4(2)
Co(3)-N(13)	2.226(6)	N(3)-Co(2)-Co(1)	88.61(16)	N(22)-Co(4)-N(6)	88.7(2)
Co(3)-N(20)	2.425(6)	N(11)-Co(2)-Co(1)	88.31(17)	N(30)-Co(4)-N(6)	90.3(2)
Co(3)-N(21)	2.235(5)	N(19)-Co(2)-Co(1)	88.25(16)	N(30)-Co(4)-N(22)	177.1(2)
Co(3)-N(28)	2.223(5)	N(27)-Co(2)-Co(1)	88.22(16)	N(6)-Co(4)-Co(5)	88.97(17)
Co(3)-N(29)	2.368(6)	N(4)-Co(3)-N(5)	57.75(19)	N(14)-Co(4)-Co(5)	88.40(17)
Co(4)-Co(5)	2.3365(13)	N(4)-Co(3)-N(12)	122.58(19)	N(22)-Co(4)-Co(5)	89.55(17)
Co(4)-N(6)	1.928(6)	N(4)-Co(3)-N(20)	74.26(19)	N(30)-Co(4)-Co(5)	87.68(16)
Co(4)-N(14)	1.918(6)	N(4)-Co(3)-N(29)	92.13(19)	N(8)-Co(5)-N(24)	90.9(2)
Co(4)-N(22)	1.927(5)	N(5)-Co(3)-N(20)	91.85(19)	N(8)-Co(5)-N(32)	87.7(2)
Co(4)-N(30)	1.927(5)	N(5)-Co(3)-N(29)	75.10(19)	N(8)-Co(5)-N(34)	94.4(2)
Co(5)-N(8)	1.955(6)	N(12)-Co(3)-N(5)	165.38(19)	N(16)-Co(5)-N(8)	173.6(2)
Co(5)-N(16)	1.950(6)	N(12)-Co(3)-N(20)	75.04(19)	N(16)-Co(5)-N(24)	90.2(2)
Co(5)-N(24)	1.958(6)	N(12)-Co(3)-N(29)	118.71(19)	N(16)-Co(5)-N(32)	90.5(2)
Co(5)-N(32)	1.965(6)	N(13)-Co(3)-N(4)	168.69(19)	N(16)-Co(5)-N(34)	91.8(2)
Co(5)-N(34)	2.100(6)	N(13)-Co(3)-N(5)	124.8(2)	N(24)-Co(5)-N(32)	173.3(2)
N(1)-Co(1)-N(9)	173.0(2)	N(13)-Co(3)-N(12)	58.24(19)	N(24)-Co(5)-N(34)	92.9(2)
N(1)-Co(1)-N(25)	90.1(2)	N(13)-Co(3)-N(20)	115.50(19)	N(32)-Co(5)-N(34)	93.7(2)
N(1)-Co(1)-N(33)	93.3(2)	N(13)-Co(3)-N(21)	80.8(2)	N(8)-Co(5)-Co(4)	86.90(16)
N(9)-Co(1)-N(25)	89.7(2)	N(13)-Co(3)-N(29)	78.74(19)	N(16)-Co(5)-Co(4)	86.88(16)
N(9)-Co(1)-N(33)	93.7(2)	N(21)-Co(3)-N(4)	110.1(2)	N(24)-Co(5)-Co(4)	86.27(16)
N(17)-Co(1)-N(1)	90.7(2)	N(21)-Co(3)-N(5)	75.4(2)	N(32)-Co(5)-Co(4)	87.16(16)
N(17)-Co(1)-Co(2)	86.66(16)	N(21)-Co(3)-N(12)	91.78(19)	N(34)-Co(5)-Co(4)	178.46(18)

short and four long Co–N bonds with Co–N distances of 2.223(5)–2.294(6) Å and 2.340(6)–2.425(6) Å, respectively. The

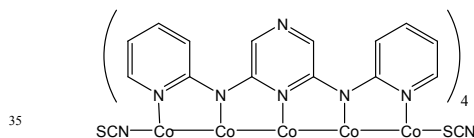
average Co(3)–N distance is 2.308(6) Å, suggesting that this cobalt(II) centre adopts a high spin state.

It is well known that ligands of oligo- $\alpha$ -pyridylamido anions favour linear metal string structure, attributed to the symmetrical optimization from the four helical ligands.<sup>[4a]</sup> All cobalt EMACs prepared to date carry nonzero metal-metal bond order with delocalized electrons along the cobalt-atom chains which are stabilized by  $\sigma$  bonding orbital of the cobalt cores.<sup>[6b,6d,10]</sup> Based on the previous studies,<sup>[4d]</sup> although the electronic structure of EMACs may be tuned by supporting ligands, it is dominated by metal character and the magnetic coupling channel is mainly through the metal centres. Intriguingly, with a missing metal centre, EMAC **2** is unable to construct a well-defined framework with the four equatorial ligands, yet **2** is very stable. Since the metal-atom chain is broken, the steric interactions arising from the crowded spacing filled by the four helical ligands is responsible for the formation and the structural stability of EMAC **2**.

Note that EMAC **2** is a neutral compound while a fully coordinated  $[\text{Co}_6(\mu_6\text{-dpznda})_4\text{X}_2]^{2+}$  would carry two positive charges. Considering the reaction medium of naphthalene and the extraction solvent of dichloromethane, neutral compounds would be more favourable than salt. This could be the origin of the formation of EMAC **2** with a missing cobalt.

The attempt to obtain high-quality crystallographic data of Compound **4** was failed due to the quick loss of the solvent during single-crystal structural measurements although a molecular structure can be refined (Scheme 4) and the structure is quite similar to its analogs of  $[\text{Co}_5(\mu_5\text{-dpzpd})_4(\text{NCS})_2]$  ( $\text{H}_2\text{dpzpd}$  =  $N,N'$ -di(pyrazin-2-yl)pyridine-2,6-diamine) and  $[\text{Co}_5(\mu_5\text{-tpda})_4(\text{NCS})_2]$  ( $\text{H}_2\text{tpda}$  = tripyridyldiamine).<sup>[6d]</sup> EMAC **4** has been subjected to the characterisation by IR, UV-Vis, NMR, and mass spectra (FAB).

**Scheme 4.** Structure of fully delocalized EMAC **4**.



### Electrochemistry

Considering tuning of metal-metal bond orders, redox properties are crucial for the potential applications of EMACs as molecular devices. Cyclic voltammetry was performed for Complexes **2** and **4** in  $\text{CH}_2\text{Cl}_2$  containing 0.1 M TBAP. **2** exhibits three redox couples at  $E_{1/2} = -1.00, +0.76,$  and  $+0.98$  V against  $E_{\text{Ag}/\text{AgCl}}$  (Fig. 2a), indicating that **2** is quite stable and very resistant to both oxidation and reduction. For **4**, the redox events taking place at  $E_{1/2} = -0.14$  and  $+0.76$  V (Fig. 3a) show that **4** is quite stable to oxidation but accessible to reduction. The electrochemical reactions are reversible and involve one-electron redox process as evidenced by thin-layer spectroelectrochemical measurements. Fig. 2b shows spectroelectrochemical spectra of the first oxidation of **2** at applied potentials ranging from  $+0.64$  to  $+0.87$  V. The absorption bands at 279, 399, 458, and 634 nm decrease associated with isosbestic points at 300, 445, 595, and 680 nm, respectively. Complex **4** is subjected to the same evaluation procedures and shows isosbestic points as well (Fig. 3b). The results demonstrate that no intermediates are produced during the redox process.

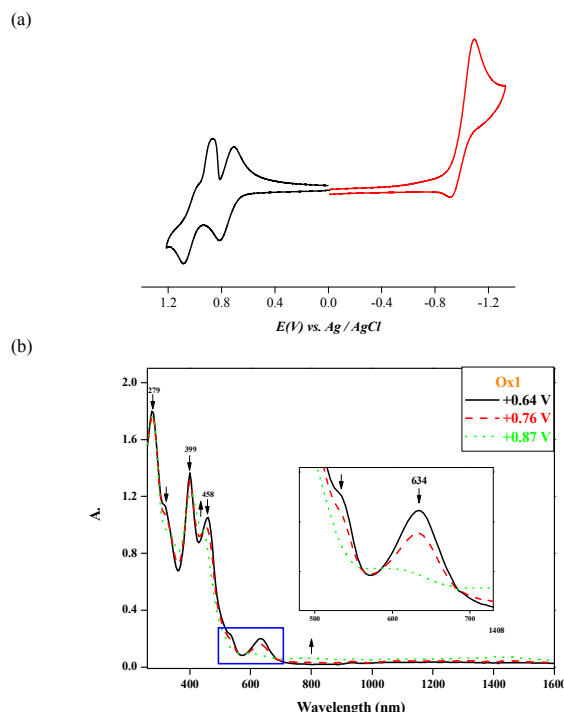


**Fig. 2** (a) Cyclic voltammogram of **2** in  $\text{CH}_2\text{Cl}_2$  containing 0.1 M TBAP. (b) Spectral changes for the first oxidation of **2** in  $\text{CH}_2\text{Cl}_2$  with 0.1 M TBAP at applied potentials from  $+0.64$  to  $+0.87$  V.

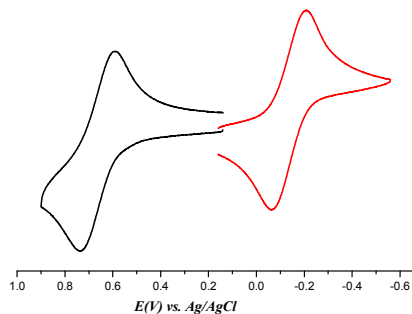
The redox potentials of **4** lie in between and are in accordance with those observed for previous obtained pentacobalt EMAC analogues,  $[\text{Co}_5(\mu_5\text{-dpzpd})_4(\text{NCS})_2]$  ( $E_{1/2} = +0.02, +0.89$  V) and  $[\text{Co}_5(\mu_5\text{-tpda})_4(\text{NCS})_2]$  ( $E_{1/2} = -0.53, +0.38, +0.88$  V).<sup>[6d,11]</sup> The first reductive wave of **2** takes place at  $-1.00$  V (*versus*  $E_{\text{Ag}/\text{AgCl}}$ ), much lower than those of the two pentacobalt EMACs. Extended Hückel MO calculations of the two pentacobalt EMACs reveal their delocalized electronic structures with relatively low energy levels for HOMO and LUMO.<sup>[6d,10c]</sup> In the case of **2**, the broken metal chain restricts electrons partially localized at the terminal di-cobalt pairs. Consequently, the energy levels of the HOMO and LUMO are higher and it is more resistant to reduction and accessible for oxidation.

### Magnetic properties

The magnetic behaviours of **2** and **4** are studied over a temperature range of 2–300 K. Plots of thermal magnetic susceptibility and magnetic moments for **2** and **4** are shown in Figs. 4 and 5, respectively. The magnetic moment for **2** at room temperature (300 K) was  $4.92 \mu_{\text{B}}$  (per molecule), corresponding to the value of quartet ground state with a significant orbital contribution (spin-only magnetic moment value for three unpaired electrons is  $3.87 \mu_{\text{B}}$ ). The result is consistent with  $4.74 \mu_{\text{B}}$  of  $[\text{Co}(\text{napy})_4(\text{ClO}_4)_2]$  ( $\text{napy} = 1,8\text{-naphthyridine}$ ), also an 8-coordinated complex.<sup>[12]</sup> The magnetic behaviour of **2** is deviated from the Curie-Weiss law. Based on the  $\sigma^2\pi^4\delta^2\delta^2\pi^4$  MO scheme for the Co–Co bonds,<sup>[9]</sup> the dicobalt(II) units are diamagnetic with paired electrons. Therefore, the magnetic contribution in **2** is attributed to the isolated  $\text{Co}^{2+}$  at the centre position. As the temperature is lowered, the  $\mu_{\text{eff}}$  values decrease

smoothly due to zero-field splitting and intermolecular interactions.

(a)



(b)

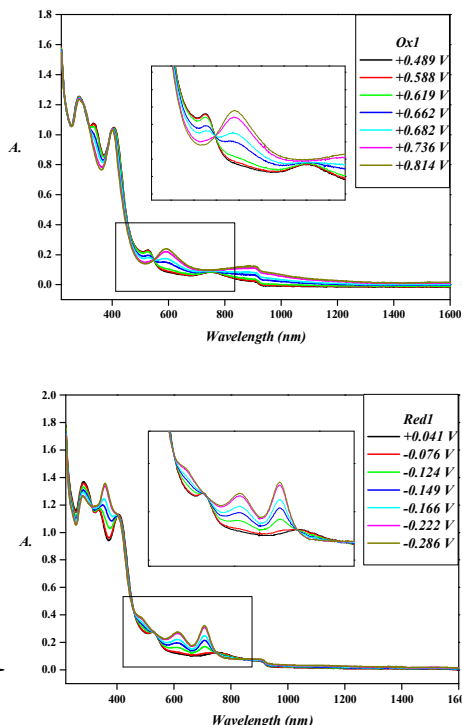


**Fig. 3** (a) Cyclic voltammogram of **4** in  $\text{CH}_2\text{Cl}_2$  with 0.1 M TBAP. (b) Spectral changes for the first oxidation of **4** in  $\text{CH}_2\text{Cl}_2$  with 0.1 M TBAP at applied potentials 20 from +0.489 to +0.814 V (upper) and from +0.041 to -0.286 V (bottom).

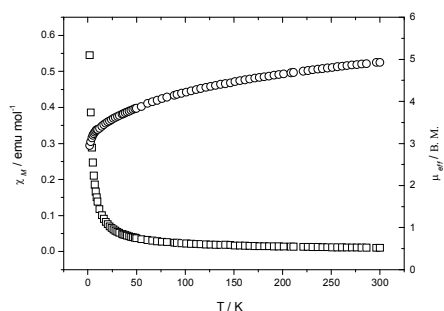


**Fig. 4** Plots of magnetic moments ( $\circ$ , right) and molar magnetic susceptibility  $\chi_M$  ( $\square$ , left) vs.  $T$  for Compound **2**.

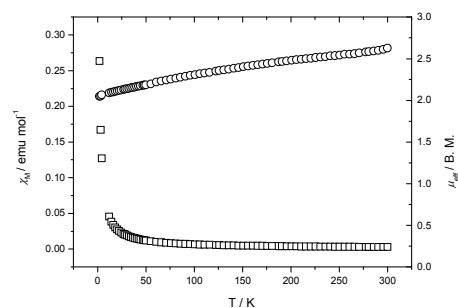


**Fig. 5** Plots of magnetic moments ( $\circ$ , right) and molar magnetic susceptibility  $\chi_M$  ( $\square$ , left) vs.  $T$  for Compound **4**.

The effective magnetic moment value for **4** at room temperature is  $2.63 \mu_B$  (per molecule). The value decreases slightly upon cooling, reaching  $2.05 \mu_B$  at 2 K. The feature of spin crossover reported for tricobalt(II) EMAC<sup>[10d,10e]</sup> is not found for **4**. The magnetic behaviour of **4** shows a spin-admixture of possible spin states of  $S = 1/2$ ,  $3/2$  and  $5/2$ , and exhibits pronounced deviation from the Curie behaviour, similar to those observed from pyrazine-modulated pentacobalt(II) and 35 heptacobalt(II) EMACs.<sup>[6b,6d]</sup>

The result of **2** is very different from those of typical cobalt(II) EMACs with a delocalized Co-atom chain. For typical cobalt(II) EMACs, the energy levels of orbitals that develop Co-Co bonds are close. For a longer cobalt(II) EMAC, the energy 40 levels become closer. Thus the small HOMO-LUMO gaps yield rich magnetic behaviours due to the different distribution of electrons. For example, it has been found the spin-crossover transition phenomenon for a tricobalt(II) EMAC, a doublet ground state for pentacobalt(II) EMACs,<sup>[10c-e]</sup> a triplet ground state for hexacobalt(II) EMACs,<sup>[7]</sup> and a spin equilibrium 45 behaviour for heptacobalt(II) EMACs.<sup>[6b]</sup> In the case of **2**, however, the  $\text{Co}^{\text{II}}_5$  chain is separated into three sections. The partially delocalized electronic structure consists of two diamagnetic dicobalt(II) units and a high-spin mononuclear cobalt(II). 50

### Molecular conductance

Quantitative single-molecule conductance of EMACs **2** and **4** are measured by the method of STM bj (scanning tunnelling microscope-based break junction) in which the molecular 55 junctions are created by repeatedly fusion and breaking contacts between the gold tip and gold substrate.<sup>[11b,13]</sup> The experiments are carried out in toluene containing *ca.* 1-mM **2** or **4**. Upon the molecular junction is created, the molecules might bridge the tip and substrate *via* the terminal sulfur and complete the measurement platform. A constant bias voltage is applied across the junction upon the tip being pulled away from the substrate. Current-distance traces can therefore be obtained and subsequently current is divided by the applied bias voltage and converted into conductance values. The left panel of Fig. 6 65 displays, for EMAC **2**, typical current-distance curves which show quantized decreases of currents corresponding to the number of EMAC molecules in the molecular junction. The panel at the right shows a histogram prepared from thousands of

traces, which was plotted against  $G_0$  (conductance quantum for the cross section of a metallic contact being only that of a single atom;  $G_0 = 2e^2/h \approx (12.9 \text{ k}\Omega)^{-1}$ ). The values of single-molecular resistance for **2** and **4** are  $15.4 (\pm 3.1) \text{ M}\Omega$  and  $12.3 (\pm 2.6) \text{ M}\Omega$ , respectively. The difference between **2** and **4** is actually small and the conductance values are comparable with  $10.0 (\pm 1.8) \text{ M}\Omega$  that of  $[\text{Co}_5(\mu_5\text{-tpda})_4(\text{NCS})_2]^{[1b]}$ . From the structural features, EMAC **2** is expected to be significantly more resistant than **4** and  $[\text{Co}_5(\mu_5\text{-tpda})_4(\text{NCS})_2]$  because of a longer Co5 core and the interruption of fully delocalized Co-Co bonds for the former. However, the difference in their conductance is not distinct. MO-mediated electron transport may provide a plausible explanation for the conductance performance of the cobalt-atom chains. The results present an interesting experimental and theoretical challenge for the future studies.

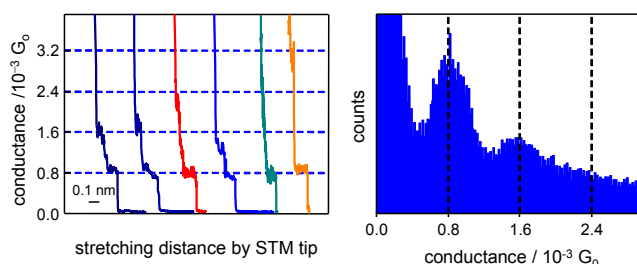


**Fig. 6** Single-molecule conductance of **2** measured by STM break junction. Left panel: typical current-distance curves acquired by stretching the molecular junctions are presented with arbitrary x-axis offset. Right panel: The conductance histogram obtained from thousands of measurements.

## Conclusions

While pyrazine-modulated tripyridyldiamine confers a fully delocalized pentacobalt EMAC of a spin admixture, through a new naphthyridine and pyrazine-containing ligand, ( $N^5, N^7$ -di(pyrazin-2-yl)-1,8-naphthyridine-2,7-diamine), a defective yet very stable pentacobalt EMAC is obtained, which has a partially delocalized and linear structure consisting of a pair of bicobalt units and an 8-coordinated cobalt isolated in the metal chain. This suggests that the contribution through  $\sigma$ - $\sigma$  bonding of the neighbouring metal centres is unnecessary for the formation and stabilisation of the EMAC framework. Magnetism study reveals that the magnetic structure consists of two diamagnetic binuclear cobalt(II) units and a high-spin mononuclear cobalt(II) complex. The electrochemical redox potentials manifest that it is more resistant to reduction and accessible for oxidation comparing with the prototypical delocalized cobalt EMACs (*i.e.*, those with oligo- $\alpha$ -pyridylamido ligands). No deterioration of EMAC **2** was found during the redox process. Conductance measurements suggest that the break of fully delocalized Co-Co bonds in EMACs does not significantly decrease the molecular conductance, an intriguing electrical behaviour deserving further attentions.

## Experimental Section

### Syntheses of compounds

**1:** 2,7-Dichloro-1,8-naphthyridine was prepared according to the literature.<sup>[7e]</sup> A mixture of 2,7-dichloro-1,8-naphthyridine (8.0 g, 40 mmol), pyrazin-2-amine (9.1 g, 96 mmol),  $\text{Pd}_2(\text{dba})_3$  (0.73 g, 0.80 mmol), dppp (0.66 g, 1.6 mmol), and  $\text{Bu}^t\text{OK}$  (13.1 g, 136 mmol) in dry toluene (350 mL) was refluxed under argon with

stirring for 4 days. The solvent was then removed. The crude product was washed with water, benzene, and methanol and recrystallized from acetone. Yield: 9.0 g, 71%; IR (KBr)  $\nu/\text{cm}^{-1} = 3444\text{w}, 3262\text{w}, 3050\text{w}, 1618\text{m}, 1508\text{s}, 1419\text{s}, 1346\text{s}, 1137\text{m}, 1007\text{m}, 828\text{m}, 796\text{m}$ ; UV-Vis (DMF)  $\lambda_{\text{max}}/\text{nm}$  ( $\epsilon/\text{dm}^3 \text{mol}^{-1} \cdot \text{cm}^{-1}$ ) = 269 ( $2.30 \times 10^4$ ), 318 ( $6.98 \times 10^3$ ), 333 ( $7.47 \times 10^3$ ), 368 ( $2.77 \times 10^4$ ), 382 ( $3.12 \times 10^4$ );  $^1\text{H}$  NMR (400 MHz,  $(\text{CD}_3)_2\text{SO}$ ):  $\delta$ 10.51 (s, 2H), 9.70–9.67 (d,  $J = 7.65$  Hz, 2H), 8.33(s, 2H), 8.21 (d,  $J = 1.55$  Hz, 2H), 8.14–8.12 (d,  $J = 5.35$  Hz, 2H), 7.58–7.56 (d,  $J = 5.42$  Hz, 2H); MS(FAB):  $m/z$  (%) 316 (45)  $[\text{M}]^+$ ; EA (%)  $\text{C}_{16}\text{H}_{12}\text{N}_8$ : calc. C 60.75, H 3.82, N 35.42; found: C 60.87, H 3.81, N 34.93%.

**2:**  $\text{H}_2\text{dpznda}$  (0.40 g, 1.3 mmol),  $\text{Bu}^t\text{OK}$  (0.34 g, 3.0 mmol), and naphthalene (20 g) were heated to boiling. Then anhydrous  $\text{CoCl}_2$  (0.30 g, 2.3 mmol) and  $\text{NaNCS}$  (0.81 mg, 10 mmol) were added to the resulted brown solution. After 8 h the solution was concentrated with a nitrogen purge to the amount of 5 mL and *n*-hexane was added to wash out the naphthalene after the system was cooled. Compound **2** was extracted with  $\text{CH}_2\text{Cl}_2$ . Dark red crystals suitable for X-ray diffraction were obtained from diffusion of hexane to a dichloromethane solution. Yield: 0.11 g, 20%; IR (KBr)  $\nu/\text{cm}^{-1} = 3440\text{w}, 2076\text{m}, 1604\text{m}, 1486\text{s}, 1448\text{s}, 1408\text{m}, 1344\text{s}, 1161\text{m}, 1147\text{m}, 1040\text{m}$ ; UV-Vis ( $\text{CH}_2\text{Cl}_2$ )  $\lambda_{\text{max}}/\text{nm}$  ( $\epsilon/\text{dm}^3 \text{mol}^{-1} \cdot \text{cm}^{-1}$ ) = 231 ( $1.15 \times 10^5$ ), 254 ( $1.13 \times 10^5$ ), 382 ( $8.07 \times 10^4$ ), 401 ( $7.10 \times 10^4$ ), 636 ( $4.30 \times 10^3$ ); MS(FAB):  $m/z$  (%) 1551 (100)  $[\text{M}-2\text{NCS}]^+$ , 1493 (20)  $[\text{Co}_4(\text{dpznda})_4]^+$ ; EA (%)  $\text{C}_{66}\text{H}_{40}\text{Co}_5\text{N}_{34}\text{S}_2 \cdot 2\text{C}_6\text{H}_{14}$ : calc. C 50.90, H 3.72, N 25.88; found: C 51.16, H 3.23, N 25.65.

**3:** The ligand  $\text{H}_2\text{dppzda}$  (**3**) was synthesized according to the literature.<sup>[14]</sup>

**4:** Anhydrous  $\text{CoCl}_2$  (169 mg, 1.30 mmol),  $\text{H}_2\text{dppzda}$  (265 mg, 1.00 mmol) and naphthalene (35 g) were mixed and heated to reflux under argon. Then a potassium *tert*-butoxide (235 mg, 2.10 mmol) solution in *n*-butyl alcohol (5 mL) was added dropwise. The reaction was continued for 15 h. The product was cooled and naphthalene was washed out by hexane. Then brown complex  $[\text{Co}_5(\mu_5\text{-dppzda})_4\text{Cl}_2]$  was extracted with *ca.* 100 mL  $\text{CH}_2\text{Cl}_2$ , and solution of  $\text{NaNCS}$  (50 mg, 0.62 mmol) in  $\text{CH}_3\text{CN}$  (2 mL) was added to the solution. The mixture was stirred for 2 d and then filtered. The filtrate was evaporated to dry and gave brown Compound **4**. The single crystals were obtained from diffusion of hexane to the  $\text{CHCl}_3$  solution. Yield: 0.36 g, 10%; IR (KBr)  $\nu/\text{cm}^{-1} = 3424\text{m}, 3092\text{m}, 2915\text{m}, 2040\text{m}, 1586\text{m}, 1494\text{m}, 1470\text{m}, 1421\text{s}, 1347\text{m}, 1156\text{m}, 1029\text{m}, 779\text{m}, 747\text{m}, 468\text{m}$ ; UV-Vis ( $\text{CH}_2\text{Cl}_2$ )  $\lambda_{\text{max}}/\text{nm}$  ( $\epsilon/\text{dm}^3 \text{mol}^{-1} \cdot \text{cm}^{-1}$ ) = 234 ( $6.79 \times 10^4$ ), 285 ( $6.82 \times 10^4$ ), 335 ( $5.90 \times 10^4$ ), 526 ( $1.31 \times 10^4$ ), 751 ( $5.06 \times 10^3$ ); MS(FAB):  $m/z$  (%) 1459 (100)  $[\text{M}-2\text{NCS}]^+$ , 1022 (20)  $[\text{Co}_4(\text{dppzda})_3]^+$ ; EA (%)  $\text{C}_{58}\text{H}_{40}\text{Co}_5\text{N}_{26}\text{S}_2 \cdot \text{CHCl}_3$ : calc. C 44.87, H 2.62, N 23.06; found: C 44.64, H 2.90, N 23.47.

### Crystal Structure Determinations

Data collection was carried out at 150(2) K using a Mo- $K\alpha$  radiation ( $\lambda = 0.71073 \text{ \AA}$ ) and a liquid nitrogen low-temperature controller on a NONIUS KappaCCD X-ray diffractometer at 150 K. Data reduction was performed on the DENZO-SMN. Semi-empirical absorption corrections were applied. All the structures were solved by using the SHELXL-97 and refined with SHELXL-97 by full-matrix least squares on  $F^2$  values.

Crystal data for  $2 \cdot 1.76\text{CH}_2\text{Cl}_2 \cdot 0.75\text{C}_4\text{H}_{10}\text{O}$ :  $\text{C}_{70.73}\text{H}_{50.94}\text{Cl}_{3.53}\text{Co}_5\text{N}_{34}\text{O}_{0.74}\text{S}_2$ ,  $M_r = 1872.73$ , triclinic, space group  $P-1$ ,  $a = 12.9626(4)$ ,  $b = 16.2465(7)$ ,  $c = 18.6106(9)$  Å,  $\alpha = 80.411(3)$ ,  $\beta = 89.948(3)$ ,  $\gamma = 88.872(3)^\circ$ ,  $V = 3863.8(3)$  Å<sup>3</sup>,  $Z = 2$ ,  $d_{\text{calcd}} = 1.610$  Mg/m<sup>3</sup>,  $\mu = 1.296$  mm<sup>-1</sup>, 32747 reflections collected, 13477 independent [ $R(\text{int}) = 0.0644$ ], goodness-of-fit on  $F^2$  1.041, final  $R1 = 0.0660$  for  $I > 2\sigma(I)$ ;  $wR2 = 0.2218$  for all data.

## 10 Acknowledgements

The authors thank the National Science Council of the Republic of China and the Nature Science Foundation of Shaanxi Province, PR China (No: 2012JM2011) for the financial support and thank Mr. Wei-Min Lee for his help with the magnetic measurements.

<sup>a</sup> School of Chemistry and Chemical Engineering, Xi'an Shiyou University, 18 Dian-zi-er Road, Xi'an, Shaanxi, P R China. Fax: +86 29 8838 3280; E-mail: wzwang@xsyu.edu.cn

<sup>b</sup> Institute of Chemical Problems of Azerbaijan Academy of Sciences, Baku-1143, Azerbaijan Republic

<sup>c</sup> Department of Chemistry, National Taiwan University, Taipei, Taiwan, ROC

<sup>d</sup> Department of Chemistry, National Chung Hsing University, Taichung, Taiwan, ROC

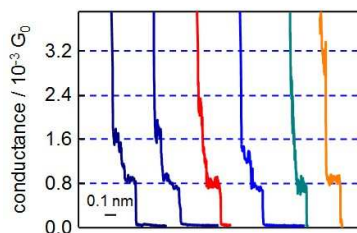
## 25 References

- (a) S.-Y. Lin, I.-W. P. Chen, C.-h. Chen, M.-H. Hsieh, C.-Y. Yeh, T.-W. Lin, Y.-H. Chen and S.-M. Peng, *J. Phys. Chem. B* 2004, **108**, 959; (b) I.-W. P. Chen, M.-D. Fu, W.-H. Tseng, J.-Y. Yu, S.-H. Wu, C.-J. Ku, C.-h. Chen and S.-M. Peng, *Angew. Chem Int. Ed.* 2006, **45**, 5814; (c) P.-C. Liu, W.-Z. Wang and S.-M. Peng, *Chem. Commun.* 2009, 4323; (d) C. Yin, G.-C. Huang, C.-K. Kuo, M.-D. Fu, H.-C. Lu, J.-H. Ke, K.-N. Shih, Y.-L. Huang, G.-H. Lee, C.-Y. Yeh, C.-h. Chen, S.-M. Peng, *J. Am. Chem. Soc.* 2008, **130**, 10090.
- T. J. Hurley and M. A. Robinson, *Inorg. Chem.* 1968, **7**, 33.
- S. Aduldecha and B. Hathaway, *Dalton Trans.* 1991, 993.
- (a) F. A. Cotton, L. M. Daniels, P. Lei, C. A. Murillo and X. Wang, *Inorg. Chem.* 2001, **40**, 2778; (b) S.-Y. Lai, T.-W. Lin, Y.-H. Chen, C.-C. Wang, G.-H. Lee, M.-H. Yang, M.-K. Leung and S.-M. Peng, *J. Am. Chem. Soc.* 1999, **121**, 250; (c) M.-Y. Huang, C.-Y. Yeh, G.-H. Lee and S.-M. Peng, *Dalton Trans.* 2006, 5683; (d) X. López, M.-Y. Huang, G.-C. Huang, S.-M. Peng, F.-Y. Li, M. Bénard and M.-M. Rohmer, *Inorg. Chem.* 2006, **45**, 9075.
- J. F. Berry, F. A. Cotton, T. Lu, C. A. Murillo and X. Wang, *Inorg. Chem.* 2003, **42**, 3595.
- (a) R. H. Ismayilov, W.-Z. Wang, R.-R. Wang, C.-Y. Yeh, G.-H. Lee and S.-M. Peng, *Chem. Commun.* 2007, 1121; (b) W.-Z. Wang, R. H. Ismayilov, G.-H. Lee, I. P.-C. Liu, C.-Y. Yeh and S.-M. Peng, *Dalton Trans.* 2007, 830; (c) R. H. Ismayilov, W.-Z. Wang, G.-H. Lee, R.-R. Wang, I. P.-C. Liu, C.-Y. Yeh, and S.-M. Peng, *Dalton Trans.* 2007, 2898; (d) W.-Z. Wang, R. H. Ismayilov, R.-R. Wang, Y.-L. Huang, C.-Y. Yeh, G.-H. Lee and S.-M. Peng, *Dalton Trans.* 2008, 6808.
- (a) C.-H. Chien, J.-C. Chang, C.-Y. Yeh, G.-H. Lee, J.-M. Fang, Y. Song and S.-M. Peng, *Dalton Trans.* 2006, 3249; (b) C.-H. Chien, J.-C. Chang, C.-Y. Yeh, G.-H. Lee, J.-M. Fang and S.-M. Peng, *Dalton Trans.* 2006, 2106; (c) T.-B. Tsao, S.-S. Luo, C.-Y. Yeh, G.-H. Lee and S.-M. Peng, *Polyhedron*. 2007, 3833; (d) I. P.-C. Liu, M. Bénard, H. Hasanov, I.-W. P. Chen, W.-H. Tseng, M.-D. Fu, M.-M. Rohmer, C.-H. Chen, G.-H. Lee and S.-M. Peng, *Chem. Eur. J.* 2007, 8667; (e) R. H. Ismayilov, W.-Z. Wang, R.-R. Wang, Y.-L. Huang, C.-Y. Yeh, G.-H. Lee and S.-M. Peng, *Eur. J. Inorg. Chem.* 2008, 4290; (f) R. H. Ismayilov, W.-Z. Wang, G.-H. Lee, C.-Y. Yeh, S.-A. Hua, Y. Song, M.-M. Rohmer, M. Bnard, and S.-M. Peng, *Angew. Chem. Int. Ed.* 2011, **50**, 2045.
- (a) P. Kiehl, M.-M. Rohmer, M. Benard M, *Inorg. Chem.* 2004, **43**, 3151; (b) J. F. Berry, F. A. Cotton and C. A. Murillo, *Dalton Trans.* 2003, 3015; (c) Y.-M. Huang, S.-H. Lai, S. J. Lee, and I.-C. Chen, C. L. Huang, S.-M. Peng, W.-Z. Wang, *J. Phys. Chem. C* 2011, **115**, 2454; (d) K.-N. Shih, M.-J. Huang, H.-C. Lu, M.-D. Fu, C.-K. Kuo, G.-C. Huang, G.-H. Lee, C.-h. Chen and S.-M. Peng, *Chem. Commun.* 2010, 1338; (e) V. P. Georgiev and J. E. McGrady, *J. Am. Chem. Soc.* 2011, **133**, 12590.
- F. A. Cotton and R. Poli, *Inorg. Chem.* 1987, **26**, 3652.
- (a) R. Clérac, F. A. Cotton, L. M. Daniels, K. R. Dunbar, C. A. Murillo and X. Wang, *Inorg. Chem.* 2001, **40**, 1256; (b) E.-C. Yang, M.-C. Cheng, M.-S. Tsai, and S.-M. Peng, *Chem. Commun.* 1994, 2377. (c) C.-Y. Yeh, C.-H. Chou, K.-C. Pan, C.-C. Wang, G.-H. Lee, Y. O. Su and S.-M. Peng, *Dalton Trans.* 2002, 2670. (d) R. Clérac, F. A. Cotton, L. M. Daniels, K. R. Dunbar, K. Kirschbaum, C. A. Murillo, A. A. Pinkerton, A. J. Schutz and X. Wang, *J. Am. Chem. Soc.* 2000, **122**, 6226; (e) D. A. Pantazis, C. A. Murillo and J. E. McGrady, *Dalton Trans.*, 2008, 608.
- C.-Y. Yeh, C.-C. Wang, C.-h. Chen and S.-M. Peng, in *Redox Systems Under Nano-Space Control*, (Ed: T. Hirao), Springer, Germany, 2006, Ch. 5.
- R. L. Bodner and D. G. Hendricker, *Inorg. Chem.* 1973, **12**, 33.
- (a) B. Xu, N. J. Tao, *Science* 2003, **301**, 1221. (b) X. Li, J. He, J. Hihath, B. Xu, S. M. Lindsay, N. J. Tao, *J. Am. Chem. Soc.* 2006, **128**, 2135.
- R. H. Ismayilov, W.-Z. Wang, G.-H. Lee, and S.-M. Peng, *Dalton Trans.* 2006, 478.

**Table of contents entry**

Wen-Zhen Wang,\* Yang Wu, Rayyat  
H. Ismayilov, Juao-Hui Kuo,  
Chen-Yu Yeh, Hsuan-Wei Lee,  
Ming-Dung Fu, Chun-hsien Chen,\*  
Gene-Hsiang Lee, and Shie-Ming  
Peng\*

**Magnetic and conductive study on  
a stable defective extended cobalt  
atom chain**



A defective extended cobalt atom chain complex has been synthesized and the magnetism and conductance are studied. The formation and the electron transporting pathway of EMACs were investigated.